Aspects of Chaos in Heavy Ion Reactions Close to a Potential Barrier

C. H. Dasso, M. Gallardo [a] and M. Saraceno [b]

The Niels Bohr Institute, University of Copenhage
Blegdamsvej 17, DK-2100 Copenhagen Ø, Denmark

[a] *Departamento de Física Atómica, Molecular y Nuclear*
Universidad de Sevilla, Apdo. 1065, E-41080 Sevilla, Spaán

[b] *Departamento de Física, Cornisión Nacional de Energia Atórnica*
Av. del Libertador 8250, Buenos Aires, Argentina

Received February 2, 1994

We investigate the occurrence of chaotic behaviour in the context of heavy ion reactions at energies close to the Coulomb barrier. At the classical level the presence of chaos is very natural as soon as a significant coupling arises between the relative motion and some collective degree of freedom. At the quantum level the signatures of chaotic behaviour are more elusive, but we are able to find their emergent role by considering Husimi transforms of the S-matrix. The method is rather simple and of general applicability.

I. Introduction

In this paper we will review a recent analysis that we have undertaken about the relevance of chaotic scattering in heavy ion reactions[1-2]. Our aim is here to introduce the main points and methods in a short and informal presrntation that might appeal to the nuclear reaction specialist who does not want to follow in full detail the intricacy of the modern description of chaotic behaviour (see e.g. Ref. [3] and other references quoted in Refs. [1-2]).

The understanding of nuclear dynamics usually goes through *a classical* step involving some phenomenological degree of freedom. Thus rotations, surface vibrations, heavy ion reactions, rotations in gauge space, etc., provide classical images appropriate for the detailed descripiion of how nuclei behave. As soon as two or more such degrees of freedom are significantly coupled we expect that chaotic motion will appear, usually inextricably mixed with regular behaviour. Therefore, classical chaotic motion should be a very common occurrence in nuclear physics, and should appear both for bound and scattering situations in regions of phase space *close* to *separatrices.* In the scattering of heavy ions the separatrix occurs as the phase space trajectory at the top of the Coulomb or centrifugal barriers, and therefore any coupling to other degrees of freedom will result in a breakup of this separatrix into a chaotic region. It is then quite relevant to investigate the effects, if any, that this simple realization has in our description and understanding of the all-important phenomena that occur in the vicinity of a potential barrier.

Our wording above has been purposefully cautíous because, although the presence of classical chaotic motion is almost unavoidable, the correct description of nuclear scattering is quantum mechanical and the correspondence is far from trivial. In fact, it is still an open question how the principle of correspondence works in detail when the classical motion is chaotic.

The standard theoretical description of a scattering problem coupled to some other degree of freedom is a coupled channel calculation. These have been performed with great sophistication and computational complexity and there is no doubt that they provide the best available description of experimental data. The

presence or absence of chaos is irrelevant to these calculations. However the interpretation that one gives to their results can be greatly enhanced if a good knowledge of the underlying classical motion exist.

II. Formulation of the Problem

We consider the coupling of the relative motion of two ions to an intrinsic harmonic mode, as expressed by an effective hamiltonian of the form

$$H^{(\ell)}(r,p,\mathrm{a},\Pi) = H^{(\ell)}_{rel}(r,p) + H_{int}(\alpha,\Pi) + V_{coup}(\alpha,r)\ . \tag{1}$$

Here r is the distance between the centers of mass of the colliding systems and a is the dimensionless variable that measures the amplitude of the vibrational motion. The variables p, Π are, respectively, their conjugate momenta. Using m for the reduced mass and C and D for the restoring force and mass parameters associated with the mode we take

$$H^{(\ell)}_{rel}(r,p) = \frac{p^2}{2m} + \frac{\ell(\ell+1)\hbar^2}{2mr^2} + U(r)\ , \tag{2}$$

$$H_{int}(\alpha,\Pi) = \frac{C\alpha^2}{2} + \frac{\Pi^2}{2D}\ . \tag{3}$$

$$V_{coup}(\alpha,r) \approx \left[-R_o\,\frac{\partial V_N}{\partial r} + \frac{3Z_1Z_2e^2}{(2\lambda+1)}\,\frac{R_o^\lambda}{r^{\lambda+1}}\right]\alpha = F(r)\alpha\ . \tag{4}$$

The real potential $U(r)$ represents the combined effects of the Coulomb interaction and of the nuclear potential $V_N(r)$, which we take here to be a Woods-Saxon version of the Christensen-Winther empirical potential of Ref. [4]. The parameters C and D are related to the energy $\hbar\omega$ and deformation parameter β of the mode by

$$C = \frac{\hbar\omega}{2\beta^2}, \qquad D = \frac{\hbar}{2\omega\beta^2}\ . \tag{5}$$

In many instances we will use the action angle variables n, φ instead of Π, a for the description of the intrinsic motion.

The coupling term V_{coup} arises from the Coulomb and surface-surface nuclear interactions between projectile and target. In leading order both these contributions are proportional to the deformation amplitudes a . Note that in (1-4) the different μ-components of a mode of multipolarity λ have been combined into an effective "monopole" amplitude. This procedure, justified in a coupled-channels approach because of their degeneracy in energy, is also appropriate for the head-on case we treat below. The actual multipolarity of the mode is taken into account in the radial dependence of the coulomb component of the form factor. These simplifications are introduced to keep the classical description as simple as possible while keeping the scales and general form of the potentials appropriate for a quantitative study.

III. Classical analysis

The equations of motion derived from the hamiltonian (1), supplemented by appropriate initial conditions, define entirely the classical evolution of the system. Because this motion is in two degrees of freedom and the couplings are non linear we expect the system to be non-integrable and therefore to show regions of chaotic behaviour. These regions will develop principally around the separatrix that occurs at the top of the barriers at each angular momentum.

We first explore the uncoupled situation. In Fig. 1 we show the potentials and phase-space trajectories for the relative and intrinsic variables. On the left the relative motion occurs in the effective ion-ion potential. The calculation corresponds to the system ^{40}Ca + ^{40}Ca and sets the centrifugal terms to zero (head-on collision). The most characteristic feature of the phase space trajectories (bottom) is the separatrix – shown in full line – which sharply divides trajectories that scatter above or below the barrier from those bound inside. The intrinsic motion, depicted on the right, is simply harmonic. Depending on the initial conditions, the total energy E_{tot} is fragmented into $E_{tot} = E_{rel} + E_{\ldots}$

and both energies are conserved separately. Therefore, it is always possible to determine if the motion is above or below the barrier (according to whether E_{rel} is larger or smaller than V_B) and this transition is sharp.

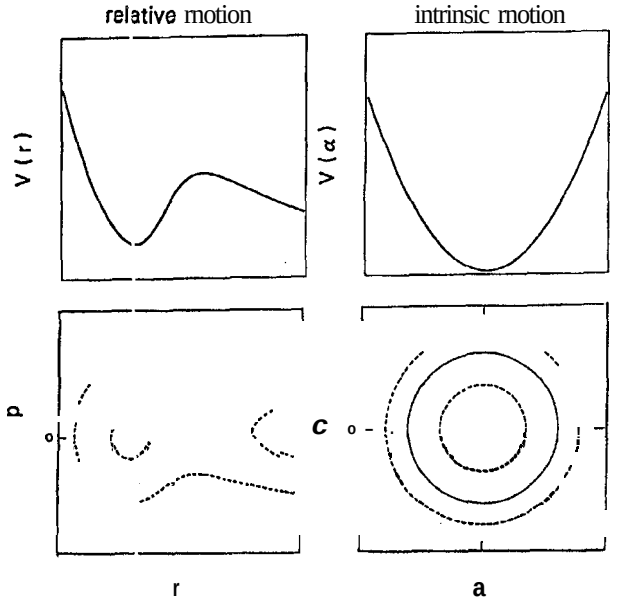

Figure 1: Qualitative representation of the potentials that determine tht: evolution of the relative motion (left) and intrinsic motion (right) in the absence of coupling. The lower frames show characteristic contour levels of the classical hamiltonians in the phase space corresponding to either degree of freedom. Scales in this figure are arbitrary and thus the equipotentials for the intrinsic hamiltonian in the ($\alpha\Pi$)-plane were chosen to appear as circles. The combination of bombarding energies and excitation energy of the harmonic mode indicated with a full line corresponds – for a given total energy E_{tot} – to the situation where the relative motion explores the separatrix.

To introduce the effects of the coupling we consider the potential surface obtained by setting all kinetic energies in eq. (1) to zero, namely

$$U_\ell(\mathrm{r},\alpha) = V_N(\mathrm{r}) + \frac{Z_1 Z_2 e^2}{\mathrm{r}} + \frac{\ell^2}{2mr^2} + \frac{C}{2}\alpha^2 + V_{coup}(r,\mathrm{a})\,. \tag{6}$$

One can think of the coupled motion as that of a particle of masses m and D in the directions r and a moving in this potential landscape. The classical motion is restricted to the region $U_\ell(r,\mathrm{a}) \leq E_{tot}$.

Contours of the function U_0 are shown in Fig. 2, for a case in which the energy of the vibrational mode is $\hbar\omega$=4 MeV and the deformation parameter is $\beta = 0.05$. The main feature of this landscape is the potential pocket connected by a "valley pass" to the asymptotic region ($\mathrm{r} \to \infty$). This pocket is responsible for the trapping of scattering trajectories and, as we shall see, for the irregular nature of the motion. It has no particular symmetries, and its general shape depends on the angular momentum and the details of the coupling form factor. The value of β sets the scale for its size. One such contour has been indicated with a full line; it corresponds to $E_{tot} = 60$ MeV, a value of the constant of the motion $H_{\ell=0}$ that will be used below.

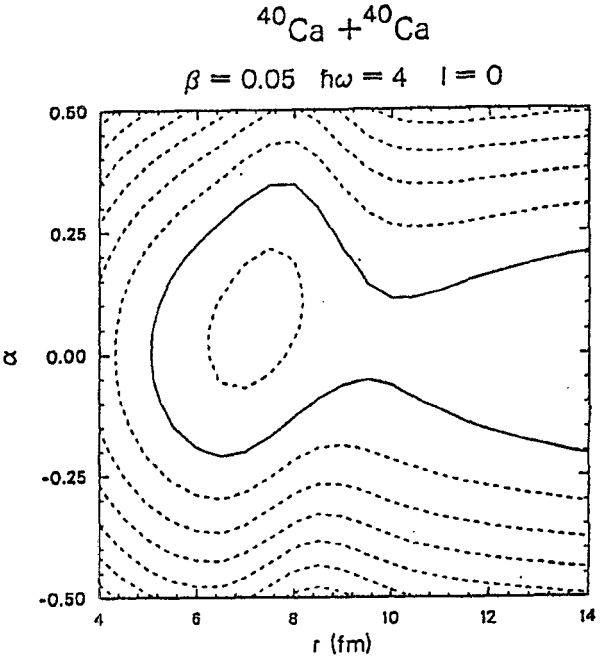

Figure 2: Contours of the potential in the $r\alpha$-plane in which the classical motion evolves in time. The calculation is for the reaction ^{40}Ca + ^{40}Ca, and corresponds to values of the parameters $\beta = 0.05$, $\hbar\omega$=4 MeV and partial wave ℓ=0. The specific contour drawn with a full line corresponds to E_{tot}=60 MeV. This value of the constant of the motion H_ℓ is the one used in the illustrations that follow in figs. 3-4, 7-8.

It is now obvious what the dynamical effect of the coupling will be. Trajectories that come in from the asymptotic region will have very different fates according to the oscillator phase with which they enter the interaction region. Very small changes in this phase can produce widely different results in the outgoing quantities as soon as trajectories bounce around several times in the pocket. The sharp separation of phase space into motion below or above the barrier, or inside and outside

the interaction region is blurred and replaced by a complex mixture of regular and irregular patterns. Without going into the technical definition of chaotic scattering (which requires an infinite amount of unstable periodic motions in the interaction region) we immediately see that a dramatic change in the organization of phase space has occurred in the vicinity of what was the separatrix of the uncoupled motion. We present two views of this structure in Fig. 3 and Fig. 4.

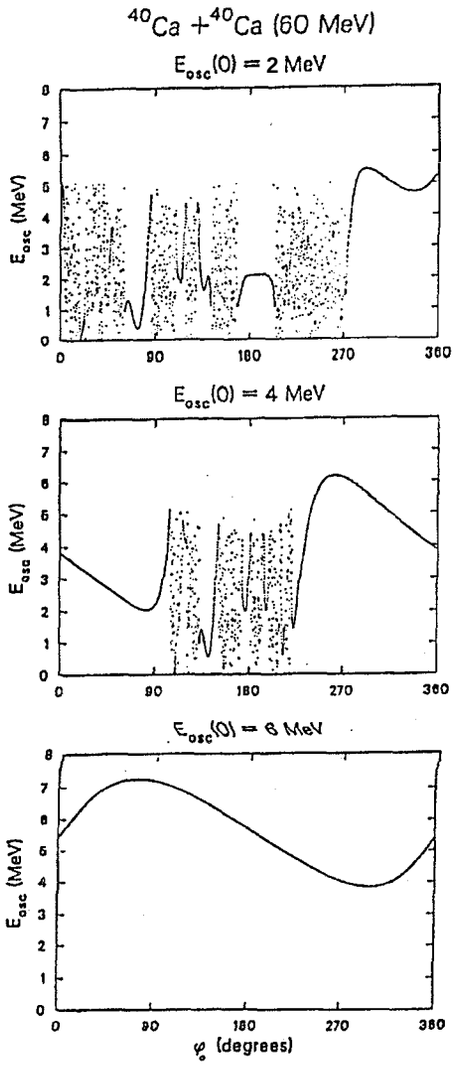

Figure 3: Final excitation energy of the harmonic mode as a function of the angle variable φ_o that specifies the initial phase of the intrinsic motion. The calculations are for the reaction $^{40}Ca + ^{40}Ca$ at $E_{tot} = 60$ MeV. Intrinsic motion parameters are $\beta = 0.1$ and $\hbar\omega = 4$ MeV. The frames are, from top to bottom, constructed using scattering trajectories corresponding to $E_{osc}(0)$ =2, 4 and 6 MeV. Notice that – as a consequence – the energy initially available to the relative motion increases going upwards in the sequence of frames.

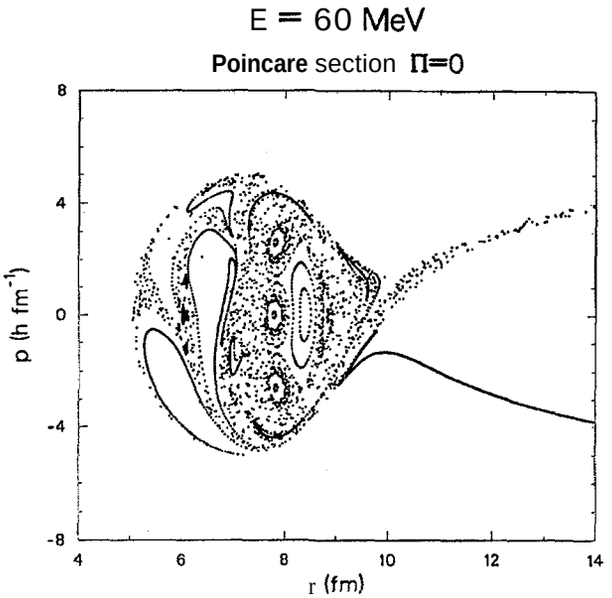

Figure 4: Poincaré section for the reaction $^{40}Ca + ^{40}Ca$ at $E_{tot} = 60$ MeV. Intrinsic motion parameters are $\beta = 0.05$ and $\hbar\omega = 4$ MeV. The plot is in the rp-plane and corresponds to cuts for Π=0, $\dot{\Pi} > 0$. The frame displays the outcome for scattering trajectories that were started asymptotically with $E_{osc}(0) = 2$ MeV, together with intersections that reveal the structure of the phase space at $E_{tot} = 60$ MeV also in a region that is unaccessible for initial conditions corresponding to scattering states. The latter identify bound motion of both regular and irregular character and were obtained by giving initial conditions inside the area.

In Fig. 3 we show the final excitation energy of the harmonic mode, E_{osc}, as a function of the angle variable φ_o. Because of total energy conservation the selected quantity represents also the kinetic energy change in the relative motion. The calculations are always for the reaction $^{40}Ca + ^{40}Ca$ at $E_{tot} = 60$ MeV. Intrinsic motion parameters are $\beta = 0.1$ and $\hbar\omega = 4$ MeV. We show the distribution for three different situations, corresponding to $E_{osc}(0) = 2$, 4, and 6 MeV. Note that the initial energy of relative motion increases as we move through the column from bottom to top. It is seen that a transition occurs in the sequence of frames. The curve for $E_{rel}(0) = 54$ MeV exhibits a smooth continuity between the input of the calculation and its outcome. At $E_{rel}(0) = 56$ MeV, however, an area of mostly erratic response has developed in the interval of φ_o between 100° and 220°. By the time $E_{rel}(0)$ has reached 58 MeV, disordered motion has set in most of the angular range. We note that these results are quite general and

have also been found, for instance, in connection with couplings to rotational degrees of freedom[5].

Fig. 4 presents a different perspective. We show the Poincaré section (at $\Pi = 0$) of the trajectories occurring in the top frame of Fig. 3. To present a complete picture of the section we have also added those trajectories that do not reach the scattering region but are bound inside the potential at the same total energy. The latter show the familiar pattern of perturbed integrable motion, with a stable trajectory (the bottom of the well) and a chain of four stable islands clearly visible. This chain is surrounded by irregular trajectories that constitute a chaotic layer which extends into the scattering region. Within this region there are many periodic trajectories which do not show up in the plot because they are unstable. However, as we will discuss later, they are mainly responsible for the structures observed in Fig. 3.

IV. Quantum analysis

The hamiltonian (1) also defines a quantum mechanical problem which is routinely solved numerically by means of a coupled channel calculation. The intrinsic motion is described in the unperturbed eigenstates

$$H_{int}|n\rangle = (\mathrm{n} + \tfrac{1}{2})\hbar\omega|n\rangle = \epsilon_n|n\rangle \qquad (7)$$

and the total wavefunction $|\Psi\rangle$ is expanded in the form

$$\langle r\alpha|\Psi\rangle = \sum_{\mathrm{n}} \chi_n(r)\langle\alpha|n\rangle \ . \qquad (8)$$

Projection into the intrinsic states leads to the set of coupled-channel differential equations

$$\left[-\frac{\hbar^2}{2m}\frac{d^2}{dr^2} + \frac{\ell(\ell+1)\hbar^2}{2mr^2} + \left[U(r) - E + \epsilon_n\right]\right]\chi_n(r) = \sum_{n'} F_{nn'}(r)\chi_{n'}(r) \ , \qquad (9)$$

where the coiipling form factors are defined by

$$F_{nn'}(r) := \int d\alpha \, \langle n|\alpha\rangle \, V_{coup}(\alpha, r) \, \langle\alpha|n'\rangle \ . \qquad (10)$$

To compare with the classical results, we solve the coupled-chanriel equations (9) for $\ell = 0$, subject to the asymptotic (screened) boundary conditions

$$\lim_{r-w} \chi_{n,ni}(r) = \delta_{n,n_i}\exp(-ik_{n_i}r) + r_{n,n_i}\exp(+ik_n r) \ , \qquad (11)$$

where $k_n = \sqrt{2m(E-\epsilon_n)/\hbar^2}$. In this expression $|n_i\rangle$ is the state in which the intrinsic system is prepared to receive the inconiing flux and therefore the index n_i labels both the resulting wavefunctions and reflection amplitudes. While in a normal situation the target would be in the ground state, $n_i = 0$, we contemplate other possibilities in order to explore the scattering matrix in its full extent. A numerical solution of the coupled-channel problem requires the truncation of the harmonic ladder to a finite number of states. The size d of the space is chosen so as to ensure that the outermost state, $|n_d\rangle$, is not significantly populated. The output of such a calculation are the channel eigenfunctions $\chi_{n_f,n_i}(r)$ and the S-matrix elements r_{n_f,n_i}.

Although these are the quantities familiar to the nuclear reaction practitioner they are not the most suitable to show explicitly the connection with the previous classical analysis. To establish this contact it is convenient to introduce a phase-space representation in terms of coherent states that displays, in a way maximally compatible with the uncertainty principle, the classical structures underlying wavefunctions and operators[6]. The Husimi transform

$$F_{n_f,n_i}(q,p) = \left| \int_{-\infty}^{\infty} \chi_{n_f,n_i}(r) \exp\left[-\frac{(r-q)^2}{2\sigma^2} + ipr \right] dr \right|^2 , \qquad (12)$$

provides a positive-definite phase space distribution that can be directly compared with the classical scattering trajectories. Notice that q takes the place of r in this representation.

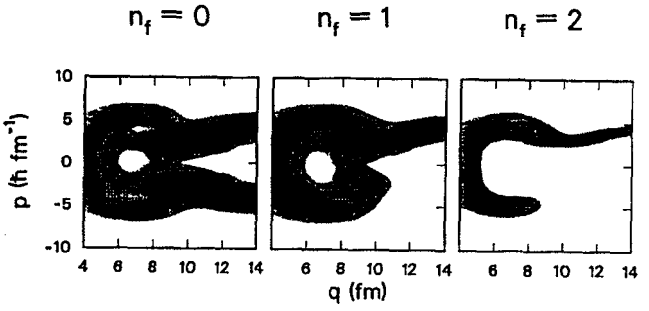

Figure 5: Phase-space representation of the coupled-channel mechanism for a total energy E = 62 MeV, above the barrier. The initial state of the intrinsic system corresponds to $n_i = 0$ and the parameters used for the intrinsic mode are $\beta = 0.05$, $\hbar\omega = 2.5$ MeV. The figure provides an overview of the process at this energy, by coilecting the contours of the functions $F_{n_i=0,n_f}$ for $n_f < 3$. For the sake of comparison the contours are displayed in an absolute gray-scale, defined so as to yield ten contours for the overall maximum.

This is shown in Fig. 5, where a classical image is given of how a coupled channel calculation (E = 62 MeV, $n_i = 0$) proceeds in phase space. The first frame shows the elastic channel with flux in both the incoming and outgoing channels. The other two frames show the inelastic channels, and how probability is gradually picked up from the interaction region to yield the outgoing flux. A region around q $\simeq$ 7 fm is avoided in all three channels indicating the presence of resonances that have a classical counterpart in the trajectories bound inside the potential (see Fig. 4). Taken together, these three frames (plus the eventual resonances) give a blurred picture of the structures present in Fig. 4. Clearly, not much detail can be expected unless the value of $\hbar$ is artificially decreased so as to explore the same classical region with an increasing number of states.

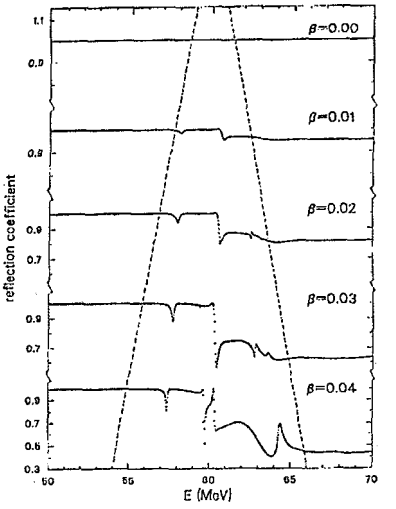

Figure 6: Probability of scattering in the ground state as a function of total energy E for different coupling strengths. The values of β are given in the figure and the intrinsic mode is defined with the same parameters as in Fig. 5. The dashed lines indicate the gradually-increasing range of energies around the Coulomb barrier where fine structures in the excitation function appear. These result from quantization within the chaotic layer and the aforementioned range roughly grows linearly with β.

Next we analyze the energy dependence of the *r*-matrix. For coupling to surface vibrations, the modulation of the barrier height extends to a range roughly equal to $V_B \pm \beta R \partial V/\partial r|_{r_B}$ [1]. This range roughly defines the extent of the region where chaotic behaviour is expected. This can be appreciated in Fig. 6, where the reflection coefficient in the entrance channel is plotted as a function of energy for several increasing values of β. As one can see, the excitation functions exhibit sharp oscillatory structures that extend gradually more and more *above the barrier* (for this case $V_B \approx 60$MeV).

[1] This result is correct only in the limit of vanishing Q-values. The finite excitation energy of the mode, $\hbar\omega > 0$, actually causes the interval to be asymmetrically distributed around v_r.

At energies below the dotted lines we have found sharp resonances (not visible in the plots) that correspond to the quantized motion inside the pocket. They are more relevant for the description of the bound states of the compound system as they are only fed by quantum tunneling. The structures in the barrier region are more interesting Eecause they represent long-lived states that quantize in the chaotic layer that has replaced the separatrix. These could be thought of as molecular resonances and they are the candidates for carrying the imprints of rhaotic rnotion. For the parameter values that we have chosen, realistic for a light heavy-ion reaction, these imprints are weak and one might have as well overlooked them (as most people doing coupled-channel calculations have rightly done so in the past). The reason for this is that nuclear vibrations involve only a few phonons and thus the situation is far from the classical limit. If the parameters were changed by softening tht: mode ($\hbar\omega \rightarrow 0$, β =const) the larger number of active channels would bring more resonances in the chaotic region. In this regime a statistical description of the resonances might be appropriate and/or correlations might show some universal behaviour.

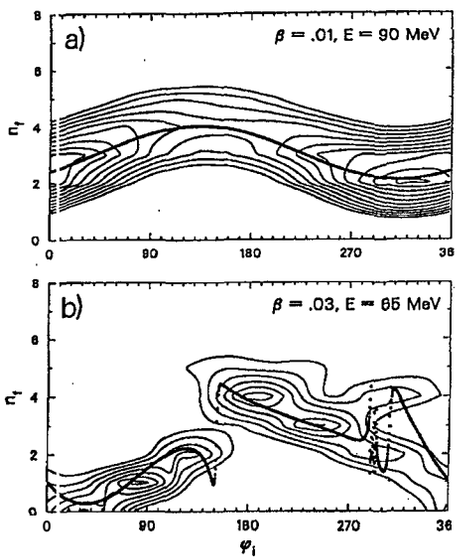

Figure 7: Final number of phonons in the harmonic mode as a function of the (arbitrary) initial phase φ_i in the $(0, \Pi)$-plane (points). The situations in a) and b) correspond, respectively, to regular and irregular regimes. The initial number of phonons is, in both cases, $n_i = 3$ and $\hbar\omega = 2.5$; other relevant parameters are quoted in the figure. Superimposed are contours of the quantal distributions $P_{n_i}(n_f, \varphi_i)$, constructed using as initial condition a coherent state that trades a small delocalization in the quantum number n_i by a sharper defiaition of the angle variable φ_i.

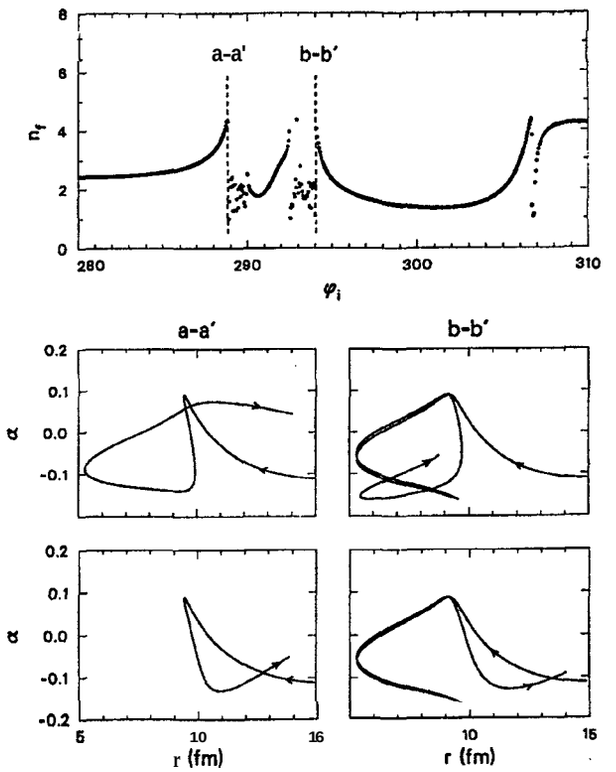

Figure 8: The top frame zooms in a high-structure region in the interval $280° \leq \varphi_i \leq 310°$ shown in Fig. 7. The enlargement reveals the emergence of similar structures at a lower scale. Discontinuities in this curve are associated with sudden, major changes in the trajectories of relative and intrinsic motion, as shown in the frames below for the specific cases a-a', b-b' in a projection on the (07)-plane.

To conclude this study we show that, even at the low quantum numbers involved in our case, one can construct quantities that reflect quite clearly, in the fully quantum rnechanical calculation, the emergent chaotic behaviour. To this end we define a quantal counterpart to the correspondence between final number of phonons and initial phase angle that so clearly indicated irregular motion in Fig. 3. The construction, easily adapted to other cases, is just a Husimi transform of the S-matrix to a coherent state representatíon [6]), but now for the oscillator states $|n>$.

A simultaneous specification of n_i and φ_i in the initial state can best be rnet within the limitations of uncertainty by constructing the coherent state

$$|I\rangle = \sum_n \frac{I^n}{\sqrt{n!}} \exp -\frac{|I|^2}{2} |n\rangle , \qquad (13)$$

where the complex number **I** is given by

$$I(n_i, \varphi_i) = \sqrt{n_i + \tfrac{1}{2}}(\cos\varphi_i + i \sin\varphi_i). \qquad (14)$$

An amplitude for populating the quantum number n_f starting from the initial state (13) can then be constructed through

$$a_{n_i}(n_f, \varphi_i) = \sum_n \left(\frac{k_{n_f}}{k_n}\right)^{1/2} r_{n_f,n} \langle n|I(n_i, \varphi_i)\rangle . \qquad (15)$$

Contours of the probability distribution $P_{n_i}(n_f, \varphi_i) = |a_{n_i}(n_f, \varphi_i)|^2$ have been plotted in Fig. 7 for two situations in the regular (a) and chaotic (b) regimes. Superimposed in the figure are the results of the classical calculation. Even with the coarse angular resolution obtained with the interferences of a few quanta, the distribution shows a remarkable correspondence with the complex pattern that characterizes the fractal structure of the classical solutions. It is encouraging to find that the main features of the S-matrix in this representation are indeed of a classical origin and provide a clear signature of the onset of chaotic behaviour.

In Fig. 8 we study the characteristics of the motion underlying the structures observed in Fig. 7 around 280°. The top part shows a blowup of the small angular interval where chaotic behaviour is observed. **A** major change in the kind of trajectories obtained occurs at each discontinuity, and these are nested in a characteristically fractal structure [3]. Although there is a clear relationship between the purely classical and the purely quantum mechanical results the quantitative semiclassical calculation of the S matrix in terms of these trajectories would represent a major challenge.

V. Summary

In Refs. [1-2] and also in this contribution we translate some of the progress made in the study of nonlinear dynamics to the terrain of nuclear reactions. To this end we have considered the coupling of the relative motion to harmonic intrinsic modes and have used values of parameters, potentials and form factors which have the magnitude and radial dependence characteristic of actual nuclear systems.

We have discussed aspects of chaotic motion that arise in the vicinity of the coulomb and centrifugal barriers in the classical problem and explored also its quantal counterpart. An important tool for this analysis is provided by the Husimi transforms of the scattering wavefunctions and of the S-matrix. These phase-space distributions establish a point of contact between the classical and quantal descriptions and display clearly the incipient signatures of chaotic behaviour.

The S-matrix transforms probe the basic output of any coupled-channel calculation and give a sensitive test of the emerging chaotic behaviour, even when the quantum numbers involved are so small that statistical tests based of random fluctuations would prove useless. The degrees of freedom considered in this analysis were deliberately kept to a minimum, so as to maintain relative transparency in the presentation. We do hope that the concepts introduced here will prove useful in the analysis of coupled channel calculations of more complex situations.

Acknowledgements

We acknowledge the kind invitation of Sociedade Brasileira de Física during M. S. stay in Serra Negra. This work was supported in part by the grant DFG Bo 1109/1, the Heraeus Foundation, the Fundación Antorchas and the Spanish CICYT project PB92-0663.

References

1. C. H. Dasso, M. Gallardo and M. Saraceno, Nucl. Phys. **A459**, 265 (1992).
2. C.H. Dasso, M. Gallardo and M. Saraceno, to be published.

3. U. Smilansky, in Chaos and Quantum Physics, edited by J. Zinn-Justin (Eisevier, Amsterdam, 1991).

4. P. R. Christensen and **A.** Winther, Phys. Lett. **65B**, 19 (1978).

5. A. Rapisarda and M. Baldo, Phys. Rev. Lett. 66, 2581 (1991).

6. R. V. Jensen, M. M. Sanders, M. Saraceno, B. Sundaram, Phys. Rev. Lett. 63, 2771 (1989).